Duan *et al.*
Chinese Journal of Mechanical Engineering (2024) 37:101
https://doi.org/10.1186/s10033-024-01092-8

Chinese Journal of Mechanical Engineering

ORIGINAL ARTICLE

Open Access

Optimizing Oil Distributor Port for Low-Pulsation Cam-Lobe Hydraulic Motors

Yiman Duan[1], Hao Tan[1], Yu Fang[1], Zhijian Zheng[2], Junhui Zhang[1], Bing Xu[1], Qi Su[1*] and Chao Zhang[1*]

Abstract

High-end equipment always operate in low-speed and heavy-load working environments, highlighting the need for cam-lobe hydraulic motors with excellent speed stability (< 1 r/min) and ultrahigh-power rotary output (> 1 MW). The successful operation of cam-lobe hydraulic motors relies on the circulation supply of high- and low-pressure oil. However, the switching between high-/low-pressure oil controlled by the oil distributor inevitably causes an obvious pressure impact and speed pulsation, which directly reduces the speed stability of hydraulic motors. Therefore, an optimization design approach for the oil distributor port is proposed to minimize the speed pulsation of cam-lobe hydraulic motors. In the proposed approach, a simulation model that links the oil distributor port structural parameters with the hydraulic motor speed pulsation was developed to clarify the effect of the oil distributor structural parameters on speed pulsation. Then, an orthogonal analysis method was used to identify the optimized oil distributor port structural parameters while minimizing the hydraulic motor's speed pulsation as much as possible. Finally, several experiments were conducted to validate the effectiveness and accuracy of the proposed optimization design approach. The experimental results indicate that the pulsation rate of the hydraulic motor equipped with the optimized oil distributor was 62.5% lower than that of the original motor at a working pressure of 25 MPa, which is consistent with the simulation results using the proposed optimization design approach. The findings of this study offer a feasible and effective approach to guide the design optimization of the oil distributor port for low-pulsation hydraulic motors.

Keywords Engineering machinery, Hydraulic motor, Pulsation, Oil distributor port, Speed stability, Optimization design

1 Introduction

Hydraulic actuation plays a critical role in various machinery and equipment, including ships, dredgers, and shield machines [1–4]. Cam-lobe hydraulic motors, which are typical low-speed and high-torque hydraulic motors, are widely used as the core component of engineering machinery because their excellent speed stability allows for position fine-tuning and precise control of the driven devices [5–9]. If a cam-lobe hydraulic motor exhibits speed instability under its working conditions, it will easily cause vibration and fatigue fracture of the driven devices, leading to the loss of valuable driven equipment [10, 11]. Thus, reducing the speed pulsation or instability of cam-lobe hydraulic motors is an important issue.

A large number of scholars have devoted extensive efforts to design low-pulsation hydraulic motors. Some scholars have attempted to develop theoretical or simulation models to obtain the output pulsation of hydraulic motors. A non-linear dynamic theoretical model, output characteristic simulation model based on non-linear

*Correspondence:
Qi Su
suqi@zju.edu.cn
Chao Zhang
chao.zhang@zju.edu.cn
[1] State Key Laboratory of Fluid Power and Mechatronic Systems, Department of Mechanical Engineering, Zhejiang University, Hangzhou 310027, China
[2] National Intelligent Manufacturing Equipment Quality Supervision and Inspection Center, Ningbo 315800, China

Springer Open

© The Author(s) 2024. **Open Access** This article is licensed under a Creative Commons Attribution 4.0 International License, which permits use, sharing, adaptation, distribution and reproduction in any medium or format, as long as you give appropriate credit to the original author(s) and the source, provide a link to the Creative Commons licence, and indicate if changes were made. The images or other third party material in this article are included in the article's Creative Commons licence, unless indicated otherwise in a credit line to the material. If material is not included in the article's Creative Commons licence and your intended use is not permitted by statutory regulation or exceeds the permitted use, you will need to obtain permission directly from the copyright holder. To view a copy of this licence, visit http://creativecommons.org/licenses/by/4.0/.

friction, and other speed pulsation models have been developed to study the pulsation of hydraulic motors. These previous studies indicate that the output pulsation of hydraulic motors is related to several factors [12–17], which mainly consist of outer (e.g., oil pressure fluctuations and load fluctuations) and inner factors (e.g., the unreasonable design of the structure including the cam ring and the oil distributor) [18, 19]. Regarding external factors, pulsation is related to the hydraulic system. Regarding the inner factors of hydraulic motors, many scholars have focused on optimizing the cam-ring curve to develop low-pulsation hydraulic motors. A series of cam-ring curves have been designed to achieve lower speed pulsation in hydraulic motors, such as a common curve (including parabolic, sine, and equal acceleration), a modified cardioid curve, and a generalized elliptical cam-ring curve [20–23]. Several optimization design methods have been developed to design special cam-ring curves for low-pulsation hydraulic motors, including a genetic-algorithm-based optimization design method for high-order function curves and non-uniform rational spline curves [20, 23]. Except for the optimization design of the cam-ring curve, the oil distributor controls the flow direction of inputting high-pressure oil and outputting low-pressure oil to drive the hydraulic motor rotation, in which the high-/low-pressure oil switching process generates an obvious pressure impact to induce high-speed pulsation [24–26]. Therefore, oil distributor optimization is crucial for achieving the low-pulsation and low-speed stability of hydraulic motors; however, few studies have focused on this issue.

In this study, an optimized design approach for oil distributor ports is introduced to reduce the speed pulsation of a cam-lobe hydraulic motor. A hydraulic motor speed-pulsation simulation model was developed to link the oil distributor port structural parameters with the hydraulic motor speed pulsation, as described in Section 3. Based on the simulation results, an orthogonal analysis method was used to select the optimized oil distributor port, as described in Section 4. In Section 5, several speed-pulsation experiments on hydraulic motors are described to validate the effectiveness of the proposed optimization design approach. Finally, Section 6 concludes the paper.

2 Configuration and Working Principle of the Cam-Lobe Hydraulic Motor

A typical cam-lobe hydraulic motor configuration is illustrated in Figure 1, which mainly consists of an oil distributor, multiple piston assemblies (i.e., pistons and rollers), a cam ring, and a cylinder block. It is worth noting that the cylinder block is fixed, while the cam ring and oil distributor rotate to convert hydraulic energy into output torque and mechanical rotation. Rotation of the cam ring is achieved by the tangential force generated between the cam ring and piston assemblies, which is controlled by periodically supplying high-pressure oil and draining low-pressure oil from the piston chambers through the oil distributor. Thus, the oil distributor plays a critical role in regulating the flow of high-/low-pressure oil in and out of the piston chambers.

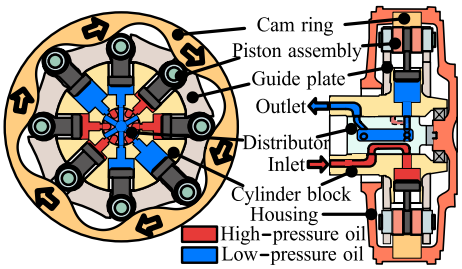

Figure 1 Configuration and working principle of the cam-lobe hydraulic motor

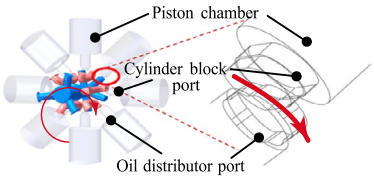

Figure 2 Oil distribution process of the cam-lobe hydraulic motor

To further illustrate the working principle of the oil distributor, the detailed high-/low-pressure oil distribution and switching process is illustrated in Figure 2. The oil distribution process can be described as that when the piston chamber is connected to the high-pressure oil port of the oil distributor through the cylinder block port, high-pressure oil flows into the piston chamber and drives the piston assemblies outward to push the roller from the inner dead center to the outer dead center. Conversely, when the piston chamber is connected to the low-pressure oil port of the oil distributor, the piston assemblies move inward, causing the roller to move from the outer dead center to the inner dead center. After the roller reaches the inner dead center of the next cycle, the piston chamber connects to the next high-pressure oil port of the oil distributor. During the high-/low-pressure oil switching process, the inevitable pressure impact causes the speed pulsations of the hydraulic motor, which is directly related to the oil distributor port configuration.

Therefore, optimizing the oil distributor port is crucial for achieving low-speed pulsation and stability in hydraulic motors.

3 Theoretical Analysis and Oil Distribution Pulsation Simulation Model

To optimize the oil distributor port for low-pulsation hydraulic motors, it is necessary to establish a relationship between the structural parameters of the oil distributor port and the hydraulic motor speed pulsation, that is, an oil distribution pulsation model. The oil distribution pulsation model is primarily determined by the flow area of the oil distribution port, leakage of the oil distribution port, and kinematics of the piston assembly. Thus, in this section, the flow area of the oil distribution port, leakage of the oil distribution port, and kinematics of the piston assembly are analyzed in detail, and the oil distribution simulation model of a single-piston assembly is established based on these three aspects. According to the different positions and motion law of the piston assembly on the cam ring, the oil distribution pulsation model of the entire hydraulic motor can be established by summing the oil distribution simulation model of the single-piston assembly.

3.1 Flow Area Theoretical Analysis of the Oil Distribution Port

The basic structural parameters of the oil distributor and cylinder block ports are shown in Figure 3(a), (b), respectively. To reduce the pressure impact on the high-/low-pressure oil-switching process, an arc transition area was designed on the oil distributor port, as shown in Figure 3(a). The corresponding plane expansion view of a high- or low-pressure oil-distribution process is shown in Figure 3(c), in which the oil distributor port gradually moves through the cylinder block port. It is apparent that the flow area of the oil distribution port is equal to the intersection area between the oil distribution port and the cylinder block port, which can be calculated by integrating the contour of the intersection.

To obtain the contour of the intersection, the contours of the oil distributor and cylinder block ports are established. By considering the midpoint of each contour as its origin, two coordinate systems are established, as shown in Figure 3(a), (b). It can be seen that each contour can be established by a quarter of its entirety, as both contours are centrosymmetric shapes. A quarter of the oil distributor port contour is described by function $f(x)$, while a quarter of the cylinder block port is described by function $g(x)$, which can be respectively expressed as follows:

$$f(x)=\begin{cases} s, & 0\le x\le d-r_2,\\ \sqrt{r_2^2-(x-d+r_2)^2}+s-r_2, & d-r_2<x<d,\\ \sqrt{r_1^2-x^2}, & d\le x\le r_1, \end{cases} \tag{1}$$

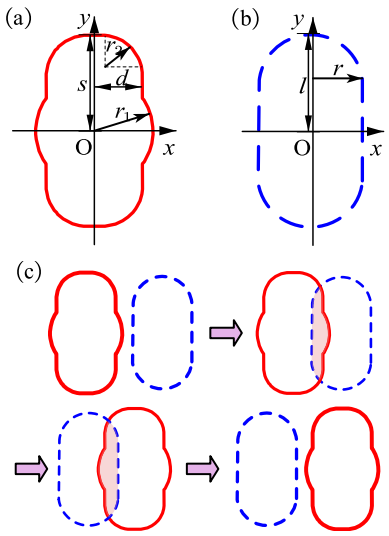

Figure 3 Shape and motion of the oil distribution port: (**a**) Oil distributor port, (**b**) Cylinder block port, (**c**) Oil-distribution process

$$g(x)=\sqrt{r^2-x^2}+l-r, 0<x<r, \tag{2}$$

where s, d, r_1, and r_2 are the half-height, width, arc transition radius, and corner radius of the oil distributor port, respectively. l and r are the semi-major and -minor axes of the cylindrical block port, respectively.

3.2 Leakage Analysis of the Piston Assembly Based on Oil Distribution

Leakage of the piston assembly occurs at two locations: the switching interface between the oil distributor and cylinder block (i.e., oil distribution pair) and the sliding interface between the piston assembly and cylinder block port (i.e., piston pair). Leakage can be considered as an eccentric annular flow with linear pressure reduction, considering the fabrication error and thermal deformation of the oil distributor. Based on the basic eccentric annular flow equation [27], the leakage of the oil distribution pair (q_1) can be expressed as:

$$q_1 = \frac{\alpha R_a h^3}{12\mu L}\Delta p\left(1 + 1.5\varepsilon^2\right), \tag{3}$$

where α is the radian of the leakage port (i.e., the high-pressure oil distribution port), R_a is the average radius ($R_a = 0.5r_a + 0.5r_b$, where r_a and r_b are the radii of the oil distributor and cylinder block center port, respectively), h is the concentric gap ($h = r_b - r_a$.), μ is the dynamic viscosity, L is the length between the oil distributor port and the outer sealing belt, Δp is the leakage pressure difference, and ε is the eccentricity ratio ($\varepsilon = e/h$, where e is the eccentric distance).

Similarly, the leakage in the piston pair (q_2) is analyzed in accordance with the leakage in the oil distribution pair, and can be expressed as:

$$q_2 = \frac{2\pi R_{a2} h_2^3}{12\mu L_2}\Delta p_2\left(1 + 1.5\varepsilon_2^2\right), \tag{4}$$

where R_{a2} is the average radius ($R_{a2} = 0.5R_2 + 0.5r_2$, where R_2 and r_2 are the radii of the piston chamber and piston, respectively), h_2 is the concentric gap ($h_3 = R_2 - r_2$.), L_3 is the leakage length, Δp_2 is the leakage pressure difference, and ε_2 is the eccentricity ratio ($\varepsilon_2 = e_2/h_2$, where e_2 is the eccentric distance).

Thus, the total leakage of the piston assembly (q_X) is the sum of the leakages in the oil distributor pair (q_1) and piston pair (q_2), and is given as follows:

$$q_X = q_1 + q_2. \tag{5}$$

3.3 Kinematics Analysis of the Piston Assembly Based on the Oil Distribution

The kinematics of the piston assembly are mainly determined by the cam-ring curve; a constant acceleration and constant deceleration cam-ring curve were used in this study. As shown in Figure 1, the piston assembly moves from the inner dead center to the outer dead center (upward movement) and then moves to the inner dead center in the next cycle (downward movement) in each acting cycle. During this upward and downward movement, the piston assembly has an equal and opposite velocity. After the piston assembly reaches the inner dead center of the next cycle, the piston assembly repeats the above motion. During the movement of the piston assembly from the inner dead center to the outer dead center, a degree of velocity is introduced to constrain the motion of the piston assembly, as illustrated in Figure 4. The velocity of the piston assembly during the piston assembly movement from the inner dead center to the outer dead center can be mathematically expressed as follows:

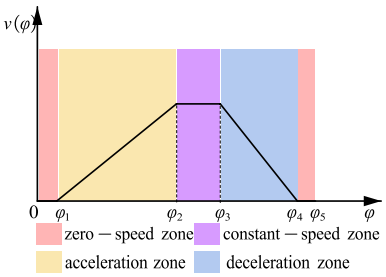

Figure 4 Velocity degree of the piston assembly under constant acceleration and constant deceleration cam-ring curves

$$v(\varphi) = \begin{cases} 0, & 0 \le \varphi < \varphi_1, \\ k_1(\varphi - \varphi_1), & \varphi_1 \le \varphi < \varphi_2, \\ k_1(\varphi_2 - \varphi_1), & \varphi_2 \le \varphi < \varphi_3, \\ k_1(\varphi_2 - \varphi_1) - k_2(\varphi - \varphi_3), & \varphi_3 \le \varphi < \varphi_4, \\ 0, & \varphi_4 \le \varphi < \varphi_5, \end{cases} \tag{6}$$

where k_1 and k_2 are the coefficients expressed as follows:

$$k_1 = \frac{2h_{io}}{(\varphi_3 - \varphi_2 + \varphi_4 - \varphi_1)(\varphi_2 - \varphi_1)}, \tag{7}$$

$$k_2 = \frac{2h_{io}}{(\varphi_3 - \varphi_2 + \varphi_4 - \varphi_1)(\varphi_4 - \varphi_3)}, \tag{8}$$

where (φ) is the rotation angle of the hydraulic motor, h_{io} is the difference in radius between the outer dead center and the inner dead center of the cam-ring curve, $(0, \varphi_1)$ and (φ_4, φ_5) are the zero-speed zone, (φ_1, φ_2), (φ_2, φ_3), and (φ_3, φ_4) are the acceleration, constant-speed, and deceleration zones, respectively.

3.4 Oil Distribution Pulsation Simulation Model

By coupling the flow area theoretical analysis of the oil distribution port (Section 3.1), leakage analysis of the piston assembly based on oil distribution (Section 3.2), and kinematics analysis of the piston assembly based on oil distribution (Section 3.3), the oil distribution pulsation simulation model of a single-piston assembly can be obtained, as shown in Figure 5(a). According to the initial positions and motion law of the piston assemblies, the oil distribution pulsation model of the hydraulic motor can also be established by summing the oil distribution simulation models of all piston assemblies, as shown in Figure 5(b). The oil distribution pulsation simulation model can be used to calculate the speed pulsation of the hydraulic motor during the subsequent optimization.

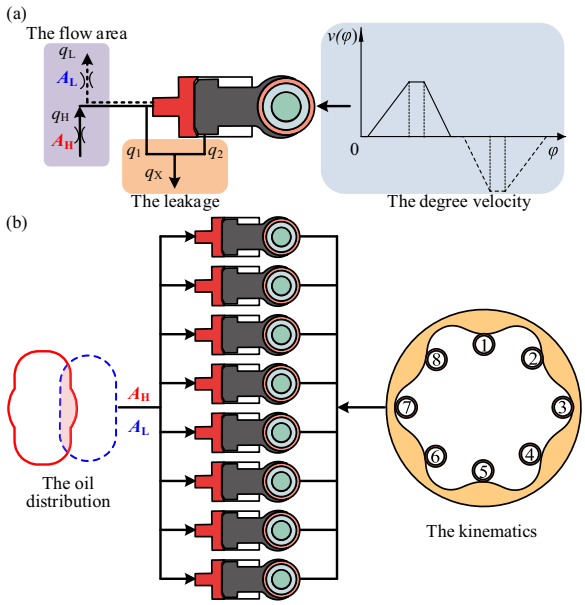

Figure 5 Simulation model: (**a**) Oil distribution pulsation simulation model for a single-piston assembly, (**b**) Oil distribution pulsation model of the hydraulic motor

Table 1 Factor level of the orthogonal analysis

Factor	A(s) (m)	B(d) (m)	C(r_1) (m)	D(r_2) (m)
Level 1	0.013	0.006	0.008	0.005
Level 2	0.0135	0.0065	0.0085	0.0055
Level 3	0.014	0.007	0.009	0.006
Level 4	0.0145	0.0075	–	–
Level 5	0.015	0.008	–	–

4 Oil Distributor Port Optimization for Low-Pulsation Hydraulic Motors

To reduce the speed pulsation of the cam-lobe hydraulic motor, an optimization design approach for the oil distributor port was developed based on the orthogonal analysis method. The orthogonal analysis method was used to evaluate the influence of the oil distributor port parameters on the speed pulsation of the hydraulic motor, thereby obtaining the optimal oil distributor port structural parameters. The orthogonal analysis process and oil distributor port parameter results are described in this section.

4.1 Orthogonal Analysis of the Oil Distributor Port Parameters

Orthogonal analysis is a scientific optimization analysis method that was used in this study to select the optimal oil distributor port parameters [28–32]. The four main oil distributor port structural parameters should be analyzed and determined, including the half-height (s), width (d), radius of the arc transition part (r_1), and radius of the elliptical groove (r_2), as indicated in Figure 3. The next step was to define the parameter values as factor levels, where one parameter value corresponds to a one-factor level for each structural parameter in Table 1. The parameter values are selected for structural parameters while considering the rationality of geometric constraints and parameters, including the number of oil distributor ports and distance between the oil distributor ports, among others. It is apparent that Factors A(s) and B(d) have five Levels, whereas Factors C(r_1) and D(r_2) have three Levels. Therefore, it is necessary to establish a mixed orthogonal analysis, as the levels of each factor are not equal; a special standard orthogonal analysis is presented in Table 2. In addition, it is worth noting that the pulsation rate values in Table 2 were calculated using the oil distribution pulsation simulation model (Figure 5(b)). The simulation parameters of the structure and working conditions are listed in Table 3.

4.2 Orthogonal Analysis Results for the Oil Distributor Port Parameters

The orthogonal analysis results for the oil distributor port parameters were divided into range and variance analyses. Range analysis can be regarded as an intuitive analysis that is used to determine three factors (including the primary factor, the optimal level of the factor, and the optimal level combination of factors). The range analysis results are presented in Table 4. In this study, the R-value was used to determine the primary factor by determining the influence of different factors on the evaluation index. The larger the R-value, the greater the influence on the pulsation rate. As can be seen in Table 4, C(r_1) has the greatest influence on the pulsation rate, followed by A(s), B(d), and D(r_2). To directly determine the influence and trend of the factors on the evaluation index, the relationship between the factor level and evaluation index was established. The pulsation rate at each factor level is shown in Figure 6. From an optimization perspective, the pulsation rate should be as small as possible. The optimal level of each factor was as follows: Factor A(s) was Level 4, Factor B(d) was Level 5, Factor C(r_1) was Level 3, and Factor D(r_2) was Level 2. However, range analysis cannot provide an accurate quantitative estimate of the factors in the order of importance. Thus, a variance analysis was introduced to determine whether there was a bias in the results, which was used to ensure the accuracy of the orthogonal analysis design, as presented in Table 5. In this study, the P-value was used to judge the significance of the different factors. The variance analysis results also

Table 2 Orthogonal analysis design, L25, and pulsation rate

Number	A	B	C	D	*s* (m)	*d* (m)	r_1 (m)	r_2 (m)	Pulsation rate
1	1	1	1	1	0.013	0.006	0.008	0.005	1.5661404
2	1	2	3	2	0.013	0.0065	0.009	0.0055	0.79965735
3	1	3	3	2	0.013	0.007	0.009	0.0055	0.79848375
4	1	4	2	3	0.013	0.0075	0.0085	0.006	1.02446695
5	1	5	2	3	0.013	0.008	0.0085	0.006	1.0378248
6	2	1	3	2	0.0135	0.006	0.009	0.0055	0.8050608
7	2	2	2	2	0.0135	0.0065	0.0085	0.0055	0.98213585
8	2	3	2	3	0.0135	0.007	0.0085	0.006	1.0150537
9	2	4	1	3	0.0135	0.0075	0.008	0.006	1.43252115
10	2	5	3	1	0.0135	0.008	0.009	0.005	0.8174325
11	3	1	2	2	0.014	0.006	0.0085	0.0055	0.9610844
12	3	2	1	3	0.014	0.0065	0.008	0.006	1.61695565
13	3	3	3	3	0.014	0.007	0.009	0.006	0.79660925
14	3	4	3	1	0.014	0.0075	0.009	0.005	0.80824745
15	3	5	2	2	0.014	0.008	0.0085	0.0055	1.0360318
16	4	1	3	3	0.0145	0.006	0.009	0.006	0.8066908
17	4	2	3	3	0.0145	0.0065	0.009	0.006	0.80014635
18	4	3	2	1	0.0145	0.007	0.0085	0.005	1.01837075
19	4	4	2	2	0.0145	0.0075	0.0085	0.0055	1.02549385
20	4	5	1	2	0.0145	0.008	0.008	0.0055	1.12215285
21	5	1	2	3	0.015	0.006	0.0085	0.006	0.96083175
22	5	2	2	1	0.015	0.0065	0.0085	0.005	0.98251075
23	5	3	1	2	0.015	0.007	0.008	0.0055	1.6366379
24	5	4	3	2	0.015	0.0075	0.009	0.0055	0.80620995
25	5	5	3	3	0.015	0.008	0.009	0.006	0.8141399

Table 3 Parameters of the structure and working conditions

Parameter	Value	Parameter	Value
Action number	6	Pump speed	1500 (r/min)
Piston number	8	Pump displacement	0.25 (L/min)
Piston stroke	0.06 (m)	Safety valve pressure	25 (MPa)
Displacement	16.34 (L/min)	Moment of inertia	300 (kg·m^2)
Roller radius	0.0425 (m)	Coefficient of viscous friction	5 (N·m/(r/min))
Piston diameter	0.085 (m)	Load torque	58500 (N·m)

show that Factor C(r_1) has the greatest influence on the results because a P-value of 0.000** indicates significant differences in the pulsation rate. The variance analysis results were consistent with those of the range analysis. According to the range and variance analyses, Factor C (i.e., the radius of the arc transition part, r_1) is the structural parameter with the greatest influence on speed pulsation. Finally, the optimized oil distributor port

Table 4 Range analysis results

Parameter	Level	A	B	C	D
K	1	5.23	5.10	7.37	5.19
	2	5.05	5.18	10.04	9.97
	3	5.22	5.27	8.05	10.31
	4	4.77	5.10	–	–
	5	5.20	4.83	–	–
K_{avg}	1	1.05	1.02	1.47	1.04
	2	1.01	1.04	1.00	1.00
	3	1.04	1.05	0.81	1.03
	4	0.95	1.02	–	–
	5	1.04	0.97	–	–
Optimal level		1	3	1	1
R		0.09	0.09	0.67	0.04
Horizontal quantity		5	5	3	3
Number of repeats per level *r*		5.0	5.0	8.0	8.0
Convert coefficient *d*		0.40	0.40	0.52	0.52
R′		0.08	0.08	0.98	0.06

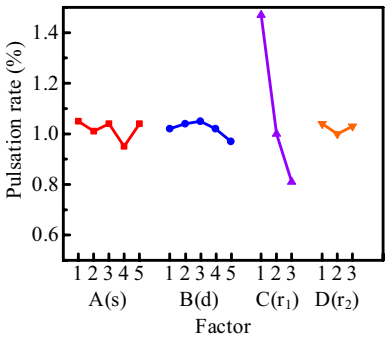

Figure 6 Pulsation rate at each factor level

Table 5 Variance analysis results

	Quadratic sum	df	Mean square	F-value	P-value
Intercept	24.666	1	24.666	2278.276	0.000**
A	0.030	4	0.007	0.690	0.613
B	0.022	4	0.005	0.499	0.737
C	1.498	2	0.749	69.186	0.000**
D	0.008	2	0.004	0.367	0.700
Residual	0.130	12	0.011		

Significance criterion: *: $p < 0.05$; **: $p < 0.01$

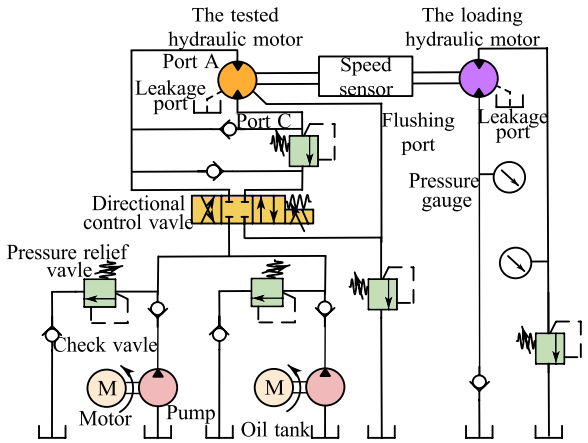

Figure 7 Pulsation rate at each factor level

structural parameters are as follows. The half-height (s): 0.0145 m; width (d): 0.008 m; radius of the arc transition part (r_1): 0.009 m; and radius of the elliptical groove (r_2): 0.0055 m.

5 Experimental Validation of the Optimized Oil Distributor Port

To validate the effectiveness of the optimization design approach, cam-lobe hydraulic motors with different oil distributors were used to test the speed pulsation. The accuracy of the hydraulic motor speed pulsation simulation model and the influence of r_1 on the hydraulic motor pulsation were validated, as discussed in this section.

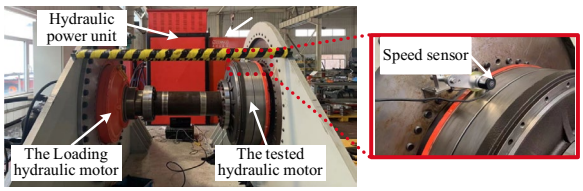

Figure 8 Test rig and hydraulic motor

5.1 Validation of the Hydraulic Motor Speed Pulsation Simulation Model

Figures 7 and 8 show the hydraulic system schematic and a photograph of the test rig, respectively, which were used to test the speed pulsation of the hydraulic motor. In the hydraulic system of the test rig, the pump delivered high-pressure oil and the directional control valve controlled the high-pressure oil flow into ports A and C of the tested hydraulic motor. The rotation of the tested hydraulic motor was controlled by periodically supplying high-pressure oil and draining low-pressure oil from the piston chambers via the oil distributor. The loading hydraulic motor was identical to that of the tested motor, which was loaded in the form of torsion. A speed sensor was used to measure the speed pulsation of the hydraulic motor and collect the speed pulsation signals using a data acquisition device.

To validate the hydraulic motor speed pulsation simulation model, three types of oil distributors with different arc transition part radii (r_1 = 0.007, 0.008, and 0.009 m) were designed and manufactured, as shown in Figure 9. These three oil distributors were installed sequentially in the tested hydraulic motor, as shown in Figure 8. Using a working pressure of 25 MPa, the speed pulsation of the hydraulic motor with three different oil distributors was measured, and the experimental speed pulsation rate was obtained by taking the average of the measured speed data and the standard error of the pulsation rate. The simulation speed pulsation rates of these three oil distributors were calculated using a hydraulic motor speed pulsation simulation model at a working pressure of 25 MPa.

Figure 10 shows a comparison between the simulated and experimental speed pulsation rates of the three oil distributors under a working pressure of 25 MPa. The comparison results indicate that the simulated speed pulsation rate was approximately consistent with the experimental speed pulsation rate, with a maximum error of less than 0.2%. This error may

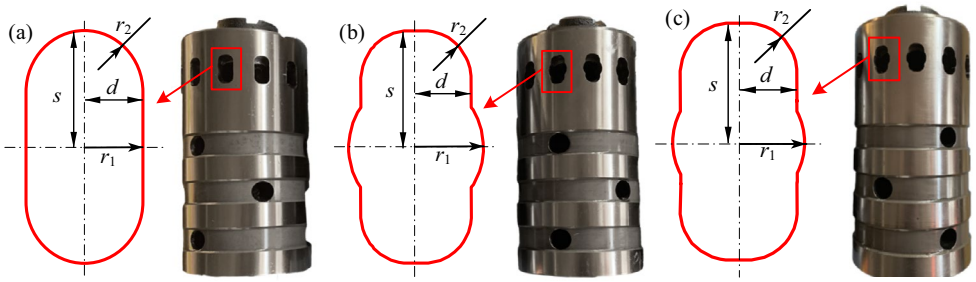

Figure 9 Oil distributors with different oil distributor ports: (**a**) $s = 0.014$ m, $d = 0.007$ m, $r_1 = 0.007$ m, $r_2 = 0.006$ m, (**b**) $s = 0.014$ m, $d = 0.007$ m, $r_1 = 0.009$ m, $r_2 = 0.006$ m, (**c**) $s = 0.014$ m, $d = 0.007$ m, $r_1 = 0.007$ m, $r_2 = 0.008$ m

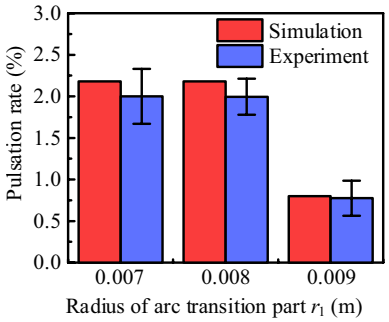

Figure 10 Pulsation comparison between the simulated and experimental results with different r_1 under 25 MPa

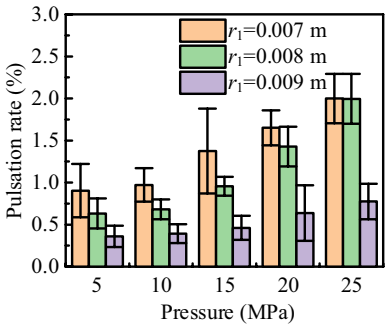

Figure 11 Pulsation rate comparison for different r_1 under different working pressures

be attributed to the machining error and cushioning effect of the coupling, which can be negligible and within an acceptable range. Thus, the hydraulic motor speed pulsation simulation model is determined to be accurate and can be used to analyze the speed pulsation and optimize other structures to reduce the pulsation of hydraulic motors.

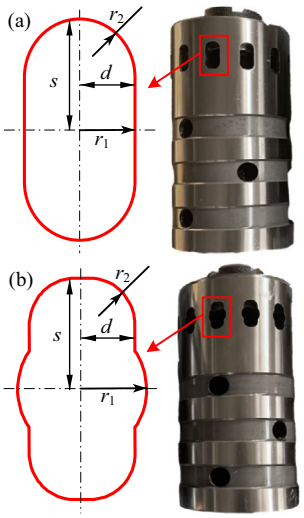

Figure 12 Original and optimized oil distributors: (**a**) $s = 0.014$ m, $d = 0.007$ m, $r_1 = 0.007$ m, $r_2 = 0.006$ m, (**b**) $s = 0.014$ m, $d = 0.007$ m, $r_1 = 0.009$ m, $r_2 = 0.006$ m

5.2 Validation of the Influence of the Arc Transition Part Radius (r_1) on the Hydraulic Motor Pulsation

To validate the influence of r_1 on hydraulic motor pulsation, the above three oil distributors with different arc transition part radii ($r_1 = 0.007$, 0.008, and 0.009 m) were used again. Figure 11 shows the speed pulsation of the hydraulic motor with different oil distributors, which was measured at different operation conditions with different inlet pressures (i.e., the pressure was varied from 5 to 25 MPa). The results show that the speed pulsation rate decreases as r_1 increases, which is consistent with the results discussed in Section 4. At a working pressure of 25 MPa, the speed pulsation rate was approximately 2% for $r_1 = 0.007$ m, while it was approximately 0.77% for $r_1 = 0.009$ m. Thus, the influence of r_1 on the hydraulic motor pulsation was validated.

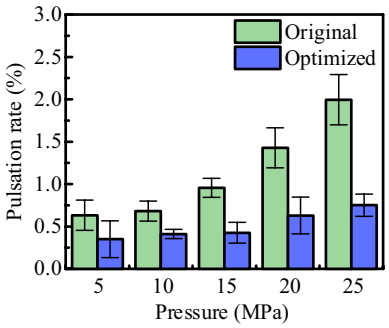

Figure 13 Pulsation comparison between the original and optimized oil distributors

5.3 Validation of the Effectiveness of the Optimization Design Approach for the Oil Distributor Port

To validate the effectiveness of the optimization design approach for the oil distributor port, original and optimized oil distributors were manufactured, as depicted in Figure 12(a), (b) respectively. The original and optimized oil distributors were installed in turn in the hydraulic motor, the speed pulsation of the hydraulic motor was measured, and the results were processed as described in Section 5.1. Figure 13 presents the speed pulsation rate of the hydraulic motors with the original and optimized oil distributors under working pressures ranging from 5 to 25 MPa. As shown in Figure 13, the speed pulsation rate of the hydraulic motor equipped with the optimized oil distributor was less than that of the hydraulic motor equipped with the original oil distributor, and the former maintained a low-speed pulsation rate (no more than 1%) under the given operating conditions. At a working pressure of 25 MPa, the speed pulsation rate of the hydraulic motor equipped with the original oil distributor was approximately 2%, whereas that of the hydraulic motor equipped with the optimized oil distributor decreased significantly to only 0.75%, indicating a 62.5% reduction. Consequently, the proposed optimization design approach for the oil distributor port was validated to be effective.

6 Conclusions

(1) A hydraulic motor speed pulsation simulation model was established and validated experimentally. The simulation speed pulsation results were consistent with the experimental results, with maximum error of less than 0.2%.

(2) The arc transition radius r_1 was identified as the primary oil distributor port structural parameter with the greatest influence on hydraulic motor pulsation. Furthermore, as r_1 increases, the hydraulic motor speed pulsation decreases.

(3) An optimized design approach for an oil distributor port was proposed and validated. The speed pulsation rate of a hydraulic motor equipped with the optimized oil distributor decreased to 0.75% at a working pressure of 25 MPa, indicating a 62.5% reduction compared with that of the original oil distributor.

Acknowledgements
Not applicable.

Authors' Contributions
YD, CZ, JZ, HT, and BX designed the research; YD, CZ, and JZ wrote the first draft of the manuscript; YD, CZ, HT, YF, and ZZ processed the corresponding experiment data, YD, CZ, JZ, BX, and QS assisted with the manuscript checking and edited the manuscript. All authors read and approved the final manuscript.

Funding
Supported by National Key R&D Program of China (Grant No. 2021YFB3400501).

Data availability
Not applicable.

Declarations

Competing Interests
The authors declare no competing financial interests.

Received: 19 August 2023 Revised: 8 July 2024 Accepted: 1 August 2024
Published online: 09 September 2024

References

[1] Z Q Wang, S F Wu, D R Gao, et al. Distribution performance analysis and experimental research on the port plate pairs of low speed high torque seawater hydraulic motor. *Chin. J. Mech. Eng.*, 2019, 32: 108.
[2] J H Zhang, Y N Shen, M Y Gan, et al. Multi-objective optimization of surface texture for the slipper/swash plate interface in EHA pumps. *Front. Mech. Eng.*, 2022, 17: 48.
[3] Y Li, X Chen, H Luo, et al. Influence of piston number on churning losses in axial piston pumps. *Chin. J. Mech. Eng.*, 2022, 35: 86.
[4] H Z Zong, J H Zhang, L Jiang, et al. Bionic lightweight design of limb leg units for hydraulic quadruped robots by additive manufacturing and topology optimization. *Bio-des. Manuf.*, 2024, 7: 1-13.
[5] S Skjong, E Pedersen. Model-based control designs for offshore hydraulic winch systems. *Ocean Engineering*, 2016, 121: 224-238.
[6] Y Fang, J H Zhang, B Xu, et al. Raising the speed limit of axial piston pumps by optimizing the suction duct. *Chin. J. Mech. Eng.*, 2021, 34: 105.
[7] Y Fang, C Zhang, C Xu, et al. Combined influence mechanism of the flexible free outer ring on contact characteristic in heavy-load cam roller bearings. *Engineering Failure Analysis*, 2024, 156: 107835.
[8] J Darnet, E Bideaux. State-of-the-art of variable displacement technologies for radial piston hydraulic machines. *Proceedings of the Bath/ASME Symposium on Fluid Power and Motion Control (FPMC) 2022*, Bath, United Kingdom, September, 2022.
[9] S L Nie, M Guo, F L Yin, et al. Research on fluid-structure interaction for piston/cylinder tribopair of seawater hydraulic axial piston pump in deep-sea environment. *Ocean Engineering*, 2021, 219: 108222.

[10] H X Zhou, J J Cao, B H Yao, et al. Hierarchical NMPC-ISMC of active heave motion compensation system for TMS-ROV recovery. *Ocean Engineering*, 2021, 239: 109834.
[11] Z Hu, E Y Wang, F Y Jia, et al. Tension-torsion fatigue behaviour of wire ropes in offshore moorings. *Ocean Engineering*, 2023, 167: 107399.
[12] R C Lin, S S Wei, X L Yuan. Low-speed instability analysis for hydraulic motor based on nonlinear dynamics. *Journal of Coal Science and Engineering*, 2010, 16: 328-332.
[13] V V Syrkin, Y F Galuza, I A Abramova, et al. Investigation of the modes of motion of a hydraulic drive with axial-piston hydraulic motors at low speeds. *Proceedings of V International Scientific and Technical Conference "Mechanical Science and Technology Update" (MSTU 2021)*, Omsk, Russia, 16-17 March, 2021.
[14] Q K Ma, X Y Wang, F Yuan, et al. Effects of the friction coefficient on the torque characteristics of a hydraulic cam-rotor vane motor. *Journal of Mechanical Science and Technology*, 2016, 30: 3507-3514.
[15] K Dasgupta, S Mandal, S Pan. Dynamic analysis of a low speed high torque hydrostatic drive using steady-state characteristics. *Mechanism and Machine Theory*, 2012, 52: 1-17.
[16] Z H Qin, K Z Wang, Y Y Li, et al. Simulation and research of one-way valve piston pump based on AMESim. *Journal of Physics Conference Series*, 2020, 1601: 062021.
[17] X Z Deng, K L Sun, H Y Zhang, et al. Modeling and simulation of the water hydraulic cylinder system based on AMESim. *Journal of Physics: Conference Series*, 2020, 1637(1): 012146.
[18] C Zhang, H Tan, Y Fang, et al. Deformation pre-compensated optimization design of cam ring for low pulsation hydraulic motors. *Journal of Zhejiang University - SCIENCE A (Applied Physics & Engineering)*, 2013, 24(2): 130-145.
[19] Z Q Wang, J B Xiang, Q Fu, et al. Study on the friction performance of textured surface on water hydraulic motor piston pair. *Tribology Transactions*, 2022, 65(2): 308-320.
[20] X L Zhang, J H Zhang, H J Zhang, et al. Optimal design of cam ring curve of cam lobe radial-piston motor. *J. Huazhong Univ. of Sci.& Tech. (Natural Science Edition)*, 2010, 49: 30-35. (in Chinese)
[21] J W Yu, K F Huang, H Luo, et al. Manipulate optimal high-order motion parameters to construct high-speed cam curve with optimized dynamic performance. *Applied Mathematics and Computation*, 2020, 371: 124953.
[22] T T N Nguyen, S Kurtenbach, M Husing, et al. A general framework for motion design of the follower in cam mechanisms by using non-uniform rational B-spline. *Mechanism and Machine Theory*, 2019, 137: 374-385.
[23] V Nguyen, D Kim. Flexible cam profile synthesis method using smoothing spline curves. *Mechanism and Machine Theory*, 2007, 42: 825-838.
[24] Z Q Wang, J B Xiang, Q Fu. Effects of wedge-shaped texture surface pair of water hydraulic motor on vibration and noise. *Journal of Central South University (Science and Technology)*, 2021, 52(9): 3174-3183. (in Chinese)
[25] X P Ouyang, X Fang, H Y Yang. An investigation into the swash plate vibration and pressure pulsation of piston pumps based on full fluid-structure interactions. *Journal of Zhejiang University-SCIENCE A*, 2016, 17(3): 202-214.
[26] C C Zhang, Y R Zang, H Y Wang, et al. Theoretical and experimental investigation on the efficiency of a novel roller piston pump. *Journal of Zhejiang University-SCIENCE A*, 2023, 24(9): 762-781.
[27] D R Gao, W Zhang. *Engineering fluid mechanics*. Beijing: Chemical Industry Press, 2014: 126-127.
[28] Y Dong, J M Liu, Y B Liu. Structure optimization of gasket based on orthogonal experiment and NSGA-II. *Science Progress*, 2021, 104(2): 657-676.
[29] W Nie, X P Cha, Q Bao, et al. Study on dust pollution suppression of mine wind-assisted spray device based on orthogonal test and CFD simulation. *Energy*, 2023, 263: 125590.
[30] J Q E, Y Zeng, Y Jin, et al. Heat dissipation investigation of the power lithium-ion battery module based on orthogonal experiment design and fuzzy grey relation analysis. *Energy*, 2020, 211: 118596.
[31] L B Ma, S Cheng, Y H Shi. Enhancing learning efficiency of brain storm optimization via orthogonal learning design. *IEEE Transactions on Systems, Man, and Cybernetics: Systems*, 2021, 51(11): 6723-6742.
[32] X H Huang, N Kang, P Coddet, et al. Analyses of the sliding wear behavior of NiTi shape memory alloys fabricated by laser powder bed fusion based on orthogonal experiments. *Wear*, 2023: 534-535.

Yiman Duan born in 1996, is currently a PhD candidate at *State Key Laboratory of Fluid Power and Mechatronic Systems, Department of Mechanical Engineering, Zhejiang University, China*. She received the B.S. degree and M.S. degree from *Yanshan University, China*, in 2019 and 2022. Her main research interests include the design and optimization of high-performance hydraulic components and system.

Hao Tan born in 1998, is currently an engineer at *Hangzhou Tooth natural Biotechnology Co., LTD, China*. He received his B.S. degree in mechanical engineering from *Xiamen University, China*, in 2020, and the M.S. degree from *Zhejiang University*, *China*, in 2023. His research interests include design and optimization of high-efficent hydraulic motors.

Yu Fang born in 1999, is currently a PhD candidate at *State Key Laboratory of Fluid Power and Mechatronic Systems, Department of Mechanical Engineering, Zhejiang University, China*. He received his B.S. degree in mechanical engineering from *Central South University, China*, in 2020. His research interests include the design and optimization of hydraulic motors.

Zhijian Zheng born in 1985, is currently a senior engineer at *the National Intelligent Manufacturing Equipment Quality Supervision & Inspection Center (Zhejiang), China*. He received the M.S. degree in 2011 and the Ph.D. degree in 2017, both from *Zhejiang Sci-Tech University*, *China*. He published more than 30 papers, and granted 12 national invention patents. He is the vice chairman of *National Hydraulic and Pneumatic Standardization Technical Committee* (SAC TC3).

Junhui Zhang born in 1983, is currently a professor at *State Key Laboratory of Fluid Power and Mechatronic Systems, Department of Mechanical Engineering, Zhejiang University, China*. He received the B.S. degree in 2007 and the Ph.D. degree in 2012, both from *Zhejiang University, China*. His research interests include high-speed hydraulic pumps/motors, and hydraulic robots. He published more than 40 papers indexed by SCI, and applied more than 20 national invention patents with 18 granted. He is supported by National Science Fund for Excellent Young Scholars.

Bing Xu born in 1971, is currently a professor and a doctoral tutor at *State Key Laboratory of Fluid Power and Mechatronic Systems, Department of Mechanical Engineering, Zhejiang University, China*. He received the Ph.D. degree in fluid power transmission and control from *Zhejiang University, China*, in 2001. He has authored or coauthored more than 200 journals and conference papers and authorized 49 patents. Prof. Xu is a chair professor of the Yangtze River Scholars Programme, and a science and technology innovation leader of the Ten Thousand Talent Programme.

Qi Su born in 1987, is currently an assistant research fellow at *State Key Laboratory of Fluid Power and Mechatronic Systems, Department of Mechanical Engineering, Zhejiang University, China*. He received the B.S. degree in 2010 and the Ph.D. degree in 2016, both from *Zhejiang University, China*. His research interests include electro-hydraulic proportional valve, electro-hydraulic servo control technology, high-speed on-off valve and system. He published more than 10 papers indexed by SCI, and won 2 first prizes of provincial and ministerial level.

Chao Zhang born in 1990, is currently a research fellow at *State Key Laboratory of Fluid Power and Mechatronic Systems, Department of Mechanical Engineering, Zhejiang University, China*. He received the B.S. degree in 2012 and the M.S. degree in 2015, from *Northwestern Polytechnical University, China*. He received the Ph.D. degree in 2019 from *University of Lyon, France*. His research interests include high-performance electro-hydrulic actuators and robotics. He published more than 40 papers indexed by SCI.